

# **In-Situ Fuel Concentration Measurement Using an IR Spark Plug Sensor by Laser Infrared Absorption Method - Application to a Rotary Engine-**

**Nobuyuki Kawahara<sup>1</sup>, Eiji Tomita<sup>2</sup>, Kenta Hayashi<sup>3</sup>,  
Michihiko Tabata<sup>4</sup>, Kouhei Iwai<sup>4</sup>, and Ryoji Kagawa<sup>4</sup>**

1: Department of Mechanical Engineering, Okayama University, Okayama, JAPAN, kawahara@mech.okayama-u.ac.jp

2: Department of Mechanical Engineering, Okayama University, Okayama, JAPAN, tomita@mech.okayama-u.ac.jp

3: Department of Mechanical Engineering, Okayama University

4: Mazda Motor Corp., Hiroshima, JAPAN

---

**Abstract** Cycle-resolved measurements of the fuel concentration near a spark plug in both a commercial spark-ignition piston engine and a commercial rotary engine were performed. An *in situ* laser infrared (IR) absorption method was developed using a spark plug sensor and a 3.392- $\mu\text{m}$  He-Ne laser as the light source. This wavelength coincided with the absorption line of hydrocarbons. The newly developed IR spark plug sensor had a higher signal-to-noise ratio than its previous version due to the optimization of its quartz lens and two optical fibers. The new sensor provided quantitative cycle-resolved fuel concentration measurements around the spark plug with a high temporal resolution. At lean preset air/fuel (A/F) ratios, fuel was mixed with the surrounding air gradually near the spark plug. Strong mixture inhomogeneities were measured during the compression stroke; the magnitude of these inhomogeneities decreased throughout the compression stroke. There was a strong correlation between the fuel concentration measured with the spark plug sensor and the combustion characteristics during the initial combustion period, which occurred faster when conditions were slightly richer than stoichiometric near the spark plug. The indicated mean effective pressure (IMEP) was slightly related to the A/F ratio near the spark plug. It was possible to measure the cycle-resolved A/F ratio near the spark plug and investigate its cycle-to-cycle fluctuations to achieve stable operation using the newly developed spark plug sensor.

---

## **1. Introduction**

Requirements of spark-ignition (SI) engine are lower fuel consumption and reduction of pollutants. The Wankel rotary engine is an alternative to a reciprocating piston engine (Heywood 1988, Stone 1999, van Basshuysen and Schäfer 2004). The advantages of this rotary engine are its compactness, higher engine speed (resulting in more power), inherent balance, and smoothness. The disadvantages are its sealing and leakage problems, lower efficiency, and higher unburned hydrocarbon emissions resulting from the flattened combustion chamber shape. Since the 1960s, several studies have attempted to improve the fuel efficiency and exhaust emissions of the Wankel rotary engine (Kanbara, et al. 2003, Jones et al. 1971, Shimamura et al. 1981, Muroki and Fujimoto 1987a, Muroki 1987b, Shimizu, et al. 1995). Recently, a new side exhaust port rotary engine has been developed (Tadasu et al. 2003, Masaki et al. 2004) that reaches higher speeds through the use of lightweight rotating parts, optimizes the intake air according to the engine speed, and uses three fuel injectors per rotor to generate high torques at both low and high engine speeds up to 9,000 rpm. The fuel injectors and spark plugs have also been upgraded to improve the fuel economy of the engine.

The flow field in the combustion chamber and the fuel concentration around the spark plugs should be optimized in commercial rotary engines to improve their fuel economy. Mixture composition of the unburned charge fundamentally influences the combustion process in a spark ignition engine. The fuel concentration around the spark plug together with the fluid motion strongly influences the combustion initiation duration. This causes cycle-to-cycle variations, which can become large in spark-ignition engines.

To better understand how to achieve both an appropriate local mixture, it is useful to have a diagnostic tool that gives the gasoline distribution in practical engines.

Several methods for measuring the fuel concentration in engines have been proposed (Zhao and Ladommatos 2001). Although fast-flame ionization detector (FID) systems that measure the instantaneous hydrocarbon concentration inside the cylinder are available, the time-lag problem is quite serious due to the sampling tube (Summers and Collings 1995). Laser diagnostics have recently been developed, including Raman scattering, Rayleigh scattering, and laser-induced fluorescence (LIF) methods (Egermann et al. 2000, Han and Steeper 2002). In particular, LIF measurements have been widely used because the signal is relatively strong and provides two-dimensional fuel concentration information at a specified time. However, these optical methods require changes in the engine combustion chamber design because of the need for optical windows, and are therefore difficult to apply to commercial rotary engines.

Recently, fuel concentrations have been measured *in situ* using infrared absorption (Hall and Koenig 1996, Yoshiyama et al. 1996, Koenig and Hall 1997, Kawamura et al. 1998, Tomita et al. 2002, Tomita et al. 2003a, Tomita et al. 2003b, Nishiyama et al. 2003, Nishiyama et al. 2004, Kawahara et al. 2006). 3.392- $\mu\text{m}$  He–Ne lasers have been used to obtain fuel concentrations for combustion diagnostics. In our previous study, a new IR optical spark plug sensor with a double-pass measurement length was developed (Nishiyama et al. 2004, Kawahara et al. 2006). The measurement accuracy was confirmed by concentration measurements of a homogeneous methane-air mixture in a compression expansion engine.

In this study, we developed spark plug sensor based on a 3.392- $\mu\text{m}$  infrared absorption technique in order to measure the fuel concentration near the spark plug in a practical spark-ignition engine. The technique was tested under firing conditions in a port-injected SI engine and Wankel rotary engine. The feasibility of the newly developed spark plug sensor is discussed for cycle-resolved measurements of the fuel concentration near a spark plug to investigate the mixture formation process in a commercial rotary engine.

## 2. Experimental Apparatus and Method

### Principle of Infrared Absorption

Assuming that light at a certain wavelength and intensity,  $I_0$ , decays to  $I$  when the light passes through a gas with concentration  $c$  (mol/cm<sup>3</sup>), along a measurement length  $L$ , then, the transmissivity,  $I/I_0$ , is expressed by Lambert–Beer's law as follows:

$$\log(I/I_0) = -\varepsilon c L \quad (1)$$

where  $\varepsilon$  denotes the molar absorption coefficient. When the measurement length  $L$  is constant, the concentration can be determined from measuring the transmissivity. The absorption bands of methane calculated using the HITRAN database (Rothman et al. 1998) are shown in Fig. 1. This shows that methane absorbs light at four wavelengths, 7.6, 3.4, 2.3, and 1.6  $\mu\text{m}$ , especially around 3.4  $\mu\text{m}$ , and each wavelength corresponds to one methane absorption line. This absorption is caused by single C–H bond stretching in the hydrocarbon molecular structure. All hydrocarbons have similar absorption characteristics because they contain many C–H bonds. A strong absorption coefficient is desired when measuring the local fuel concentration in a SI engine because of measurement length limitations. In this study, an infrared 3.392  $\mu\text{m}$  He–Ne laser was used due to its stable wavelength and output power.

The absorbance ( $1 - I/I_0$ ) of methane was calculated from the HITRAN database (Rothman et al. 1998), as shown in Fig. 2. The absorption lines are sharp when the pressure and temperature are 100 kPa and 300 K, respectively (see Fig. 2(a)). However, as the pressure and temperature increase to 2,000 kPa and 600 K, respectively, which are similar to values found in an engine just before ignition, the absorption lines merge and form a broad spectrum due to collisional broadening (see Fig. 2(b)). Because the absorbance value depends on the pressure and temperature of the methane, the fuel absorption coefficients were measured in advance at different ambient pressures and temperatures up to normal engine conditions.

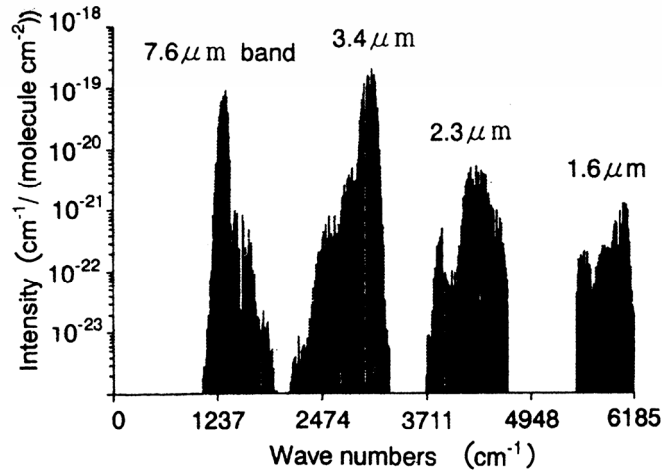


Fig. 1 Absorption lines of methane calculated with HITRAN database

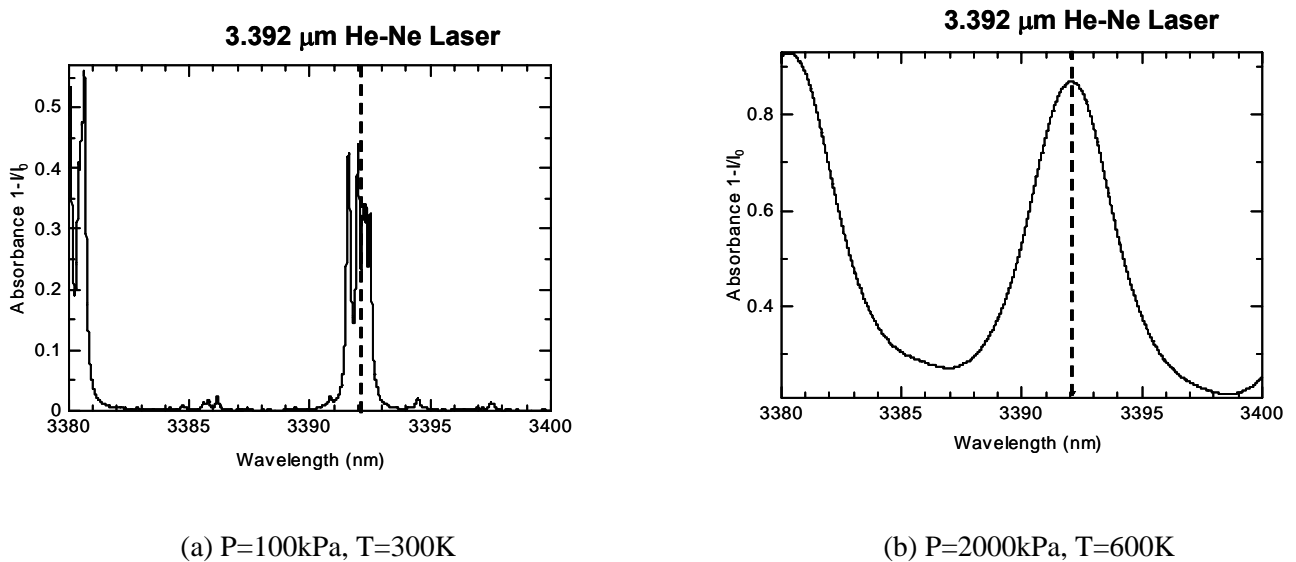


Fig. 2 Effects of surrounding pressure and temperature on absorbance of methane

### Developed Spark Plug Sensor

Figure 3 shows the optical sensor installed in a spark plug. This sensor was constructed by modifying a commercial instrumented spark plug. Consequently, it is possible to measure the fuel concentration near the spark plug under firing conditions by replacing a standard spark plug with this spark plug sensor. The optical setup consists of two optical fibers, a quartz lens, and a metal mirror. The quartz lens protects the end faces of the fibers from burned gas at high pressures and temperatures. One of the optical fibers guides light from the laser to the sensor. The light passes through the quartz lens and is reflected by the mirror. The reflected light then passes through the quartz lens again, and is transmitted to the detector through the second fiber. The measurement region is the gap between the quartz lens and the metal mirror. The measurement length is twice longer than the gap length, because the light traverses the gap in both directions. Developed IR spark plug sensor can detect the signal during some hours because of use of Ni related material as the metal mirror. It is possible to clean up the metal mirror and the quartz lens and continue the next experiments. Effect of deposits on the metal mirror or the quartz lens on the life time of measurement was not needed to consider under our experimental conditions. This newly developed IR spark plug sensor has a higher signal-to-noise ratio than a previous version due to the optimization of the quartz lens and the two optical fibers (Kawahara et al. 2006).

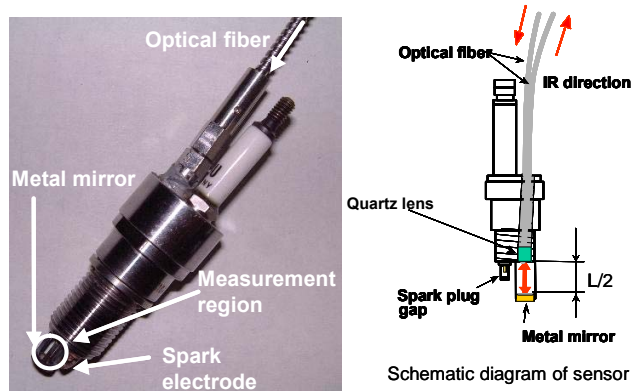


Fig.3 Schematic diagram and photograph of an IR spark plug sensor

### 3. Application to Spark-ignition piston engine

Figure 4 shows the experimental setup used to measure the concentration in a port-injected lean-burn engine employing the laser infrared absorption method with our spark plug sensor. A four-stroke cycle SI engine with a single cylinder was used to test this measurement technique; the bore and stroke were 70 and 58 mm, respectively, and the compression ratio was 9.5:1. The throttle valve was closed almost completely while idling, and the gasoline fuel was injected into the intake port using the port-injection system. The crank angle and top dead center (TDC) from a rotary encoder were used to change the spark timing and port-injection timing in the engine control unit (ECU), and were recorded using an analog/digital (A/D) converter. The in-cylinder pressure was obtained using a pressure transducer set in the spark plug. The history of the in-cylinder pressure is critical for evaluating the molar absorption coefficient of fuel using our IR sensor system.

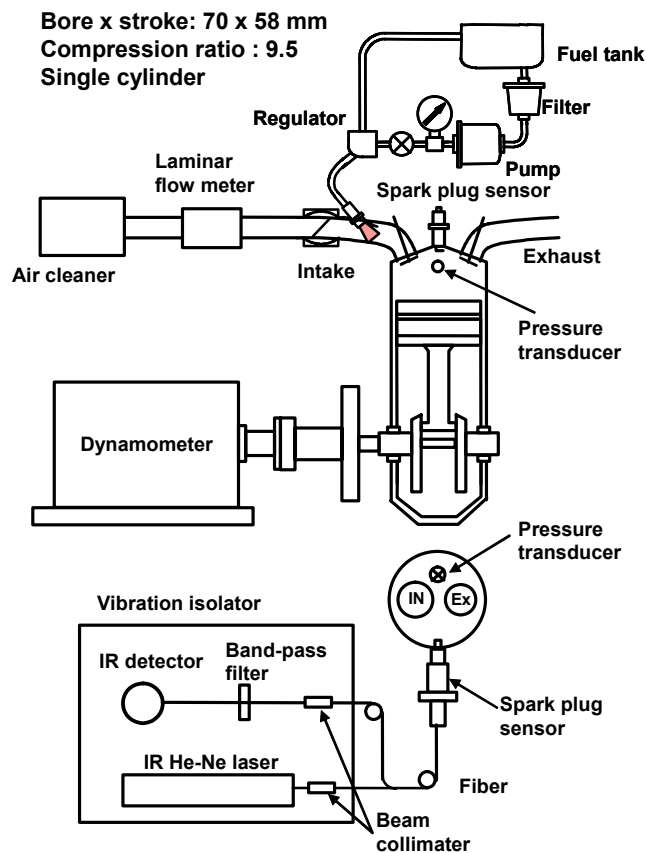


Fig. 4 Experimental set-up for spark-ignition piston engine

We investigated the mixture formation process near the spark plug using the laser infrared absorption method with a 3.392  $\mu\text{m}$  He-Ne laser as the light source, and we discuss the effect of injection timing,  $\theta_{inj}$ , on the fuel concentration near the spark plug and the relationship between the fuel concentration and combustion characteristics.

Figure 5 shows an example of the transmissivity,  $I/I_0$ , when  $(A/F)_0 = 17.0$  and  $\theta_{inj} = -30, 60,$  and  $120^\circ$  ATDC intake. These are the average results for 100 cycles. During the intake stroke, the transmissivity decreased as the fuel flowed into the cylinder from the intake port and passed near the spark plug. During the compression stroke, the transmissivity decreased as the in-cylinder volume decreased and the molar concentration of the mixture increased. With the spark, the transmissivity decreased suddenly due to the greater absorption of gasoline. After the spark, the transmissivity increased suddenly because the flame propagated through the measurement region and removed hydrocarbons. The timing of the decrease in transmissivity during the intake stroke depended largely on the injection timing. When  $\theta_{inj} = -30, 60,$  and  $120^\circ$  ATDC intake, the time at which fuel reached the spark plug was delayed because the injection timing was delayed.

Figure 6 shows the A/F ratio during the latter part of the compression stroke when  $\theta_{inj} = 120^\circ$  ATDC intake and  $(A/F)_0 = 14.7, 17.0$ . The molar concentration was converted into the A/F ratio using the mass flow of air measured by a laminar flow meter installed upstream from the intake manifold. Here, we assumed that the residual gas mixed with the fresh air homogeneously. The A/F ratio decreased and then reached at the rich concentration in comparison to  $(A/F)_0$  at the spark. Under this condition ( $\theta_{inj} = 120^\circ$  ATDC), a rich mixture remained near the spark plug. Delaying injection caused a richer fuel concentration around the the spark plug and a leaner mixture near the wall. We could determine the fuel concentration near the spark plug using our IR sensor system.

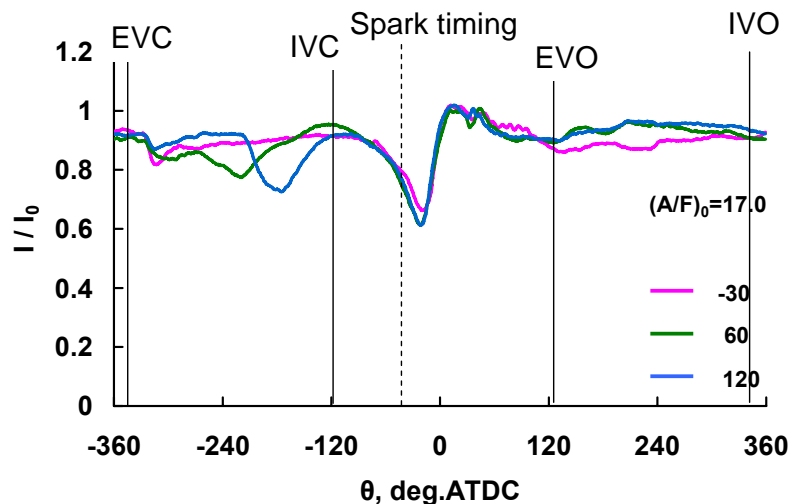


Fig. 5 Transmissivity for each injection timing

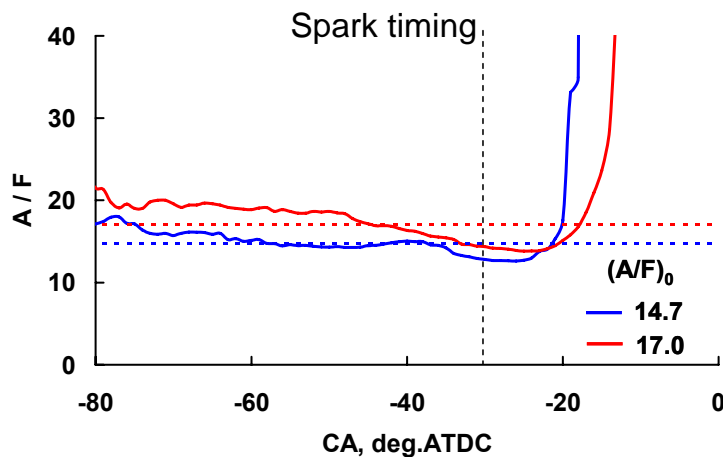


Fig. 6 Time-series of A/F ratio under the late injection condition.

The fuel concentration near the spark plug is thought to affect the stability of lean mixture combustion. Figure 7 shows the relationship between the fuel concentration near the spark plug at ignition and the coefficient of variation of the indicated mean effective pressure (IMEP),  $COV_{IMEP}$  under the condition of  $\theta_{inj} = 120^\circ$  ATDC and  $(A/F)_0$  (17.0). The A/F ratio is very important for the IMEP. Near the richer stoichiometry, IMEP indicates larger and there was a rich concentration at the spark, as shown in Fig. 6. There was a correlation between the A/F ratio and  $COV_{IMEP}$ , which decreased when a rich mixture was present at the spark. We confirmed that the fuel concentration measured with the spark plug sensor was related to the combustion characteristics of the coefficient of variation of the IMEP.

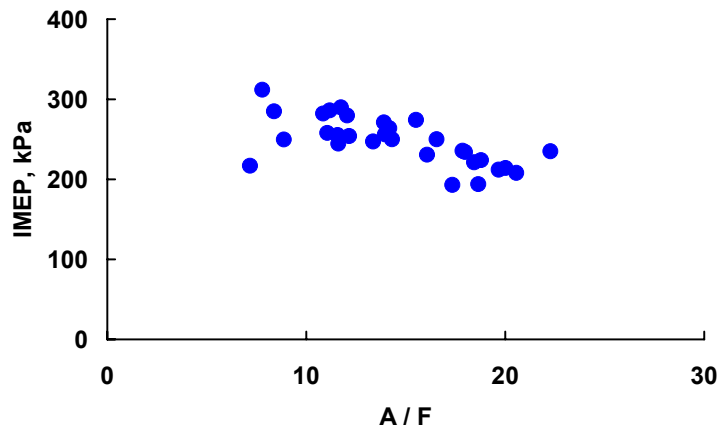


Fig. 7 Relationship between the air/fuel ratio (A/F) near the spark plug at the time of the spark and the coefficient of the IMEP variation

#### 4. Application to rotary engine

Figure 8 shows the experimental setup. The four-stroke rotary engine was essentially a naturally aspirated Mazda 13B engine (Tadasu et al. 2003, Masaki et al. 2004). This commercial rotary engine has two plug holes in one rotor housing. The pressure in the combustion chamber was measured using a pressure transducer installed on the trailing side (T) of the spark plug. The leading side (L) of the spark plug was replaced with the spark plug sensor. Figure 9 gives an example of the in-cylinder pressure history measured in the T-plug hole. This figure also shows the position of the rotor in the housing. An apex seal on the rotor edge passed through the T-plug hole when the eccentric shaft angle was  $-255$  degrees. The intake port was left open until the eccentric shaft angle was  $-205$  degrees. The mixture was ignited at  $-17$  degrees, causing the in-cylinder pressure to rise suddenly due to combustion. At 105 degrees after TDC, the next apex seal passed through the T-plug hole.

The mixture formation process near the spark plug (L-plug hole) in the rotary engine was investigated using a laser infrared absorption method. Figure 10 shows the A/F ratio during the latter part of the compression stroke. The dotted lines in each figure indicate the standard deviation of A/F ratio. The A/F ratio near the spark plug maintained a constant value at the preset  $(A/F)_0$  when  $(A/F)_0 = 13.1$  and  $14.7$ . The standard deviations at these conditions were very small. The delay from the spark timing to the sudden increase in the A/F ratio due to combustion under these conditions was roughly the same amount of elapsed time as required for 7 degree of eccentric shaft rotation. Under these conditions, the gasoline mixed with the surrounding air almost homogeneously and remained in the combustion chamber and inside the L-plug hole. However, for the leaner case,  $(A/F)_0 = 16.1$ , the A/F ratio decreased gradually before finally approaching the preset  $(A/F)_0$ . The standard deviation of the A/F ratio was larger and the elapsed time from the spark timing to the sudden increase in the A/F ratio was shorter than those of the richer cases. In the leaner case, the fuel mixed with the surrounding air gradually and strong mixture inhomogeneities were measured during the compression stroke. The magnitude of these inhomogeneities decreased throughout the compression stroke. The projected metal mirror mount of the spark plug sensor affected the fuel concentration measurements for

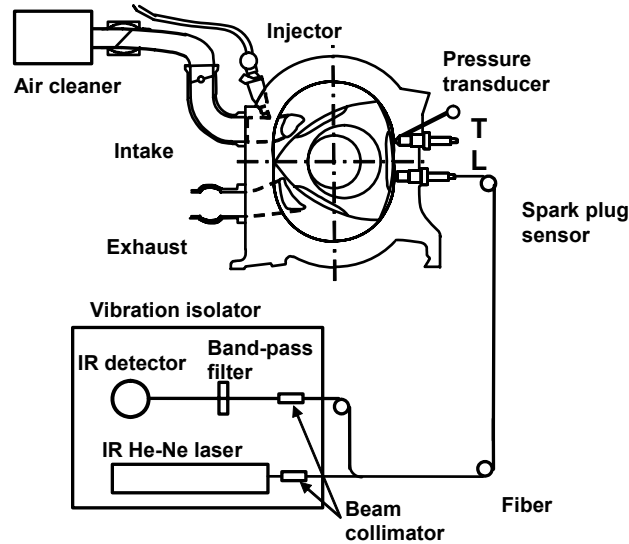


Fig. 8 Experimental setup of the rotary engine together with IR spark plug sensor system

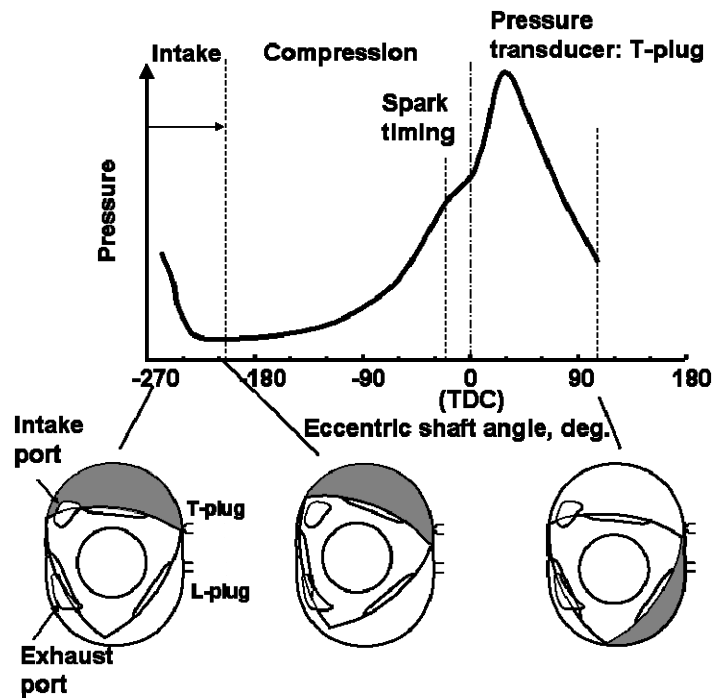


Fig. 9 Pressure history of the rotary engine with rotor position in the housing

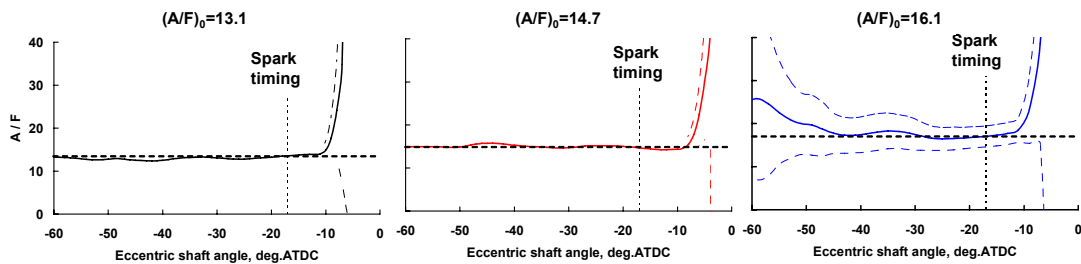
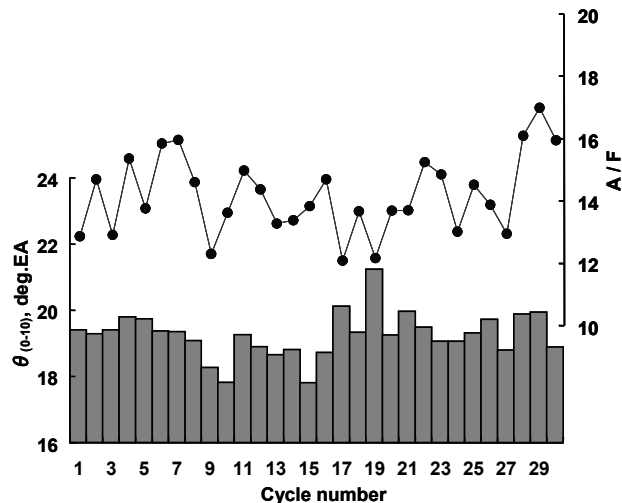


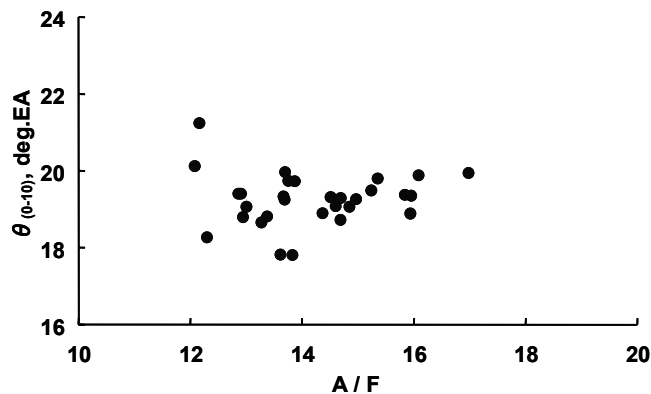
Fig. 10 Measured air/fuel ratio around the spark plug

the leaner conditions slightly. The large differences in the averaged A/F ratio at the spark timing shown in Fig. 10 demonstrated that the developed measurement system could easily distinguish between the different A/F ratios. Therefore, it was possible to quantify the fuel concentration during the compression stroke using the new spark plug sensor. Fuel concentration measurements potentially allow us to understand differences in the mixture formation processes inside the combustion chamber and around the spark plug caused by the preset  $(A/F)_0$ .

Next, cycle-to-cycle fluctuations of the charge distribution introduce severe restrictions on combustion and engine performance. In particular, the fuel concentration near the spark plug is thought to affect the initial stages of combustion and the stability of lean mixture combustion. Figure 11(a) gives the cycle-to-cycle fluctuations of the initial combustion period and the A/F ratio at the spark timing under the condition  $(A/F)_0 = 14.7$ , while Fig. 11(b) shows the relationship between the measured A/F ratio and the initial combustion period,  $\theta_{(0-10)}$ , which denotes the period from a spark timing until 10% of the mass was burned. From cycles 5 to 10 and 11 to 15, the initial combustion period decreased gradually with richer fuel concentrations. Since the A/F ratio increased at cycle 10, the initial combustion period became longer at cycle 11. The former cycle often had a direct effect on the next cycle. Leaner A/F ratios had slightly longer initial combustion periods. The shortest initial combustion period occurred for a slightly richer than stoichiometric mixture (approximately A/F = 13.0) at the spark timing. There was evidence that the A/F ratio near the spark plug affected the initial combustion period.



(a) Cyclic fluctuations of the initial combustion period and the A/F ratio around the spark plug



(b) Relationship between the initial combustion period and the A/F ratio around the spark plug

Fig. 11 Effect of the A/F ratio at the spark timing on the initial combustion period ( $(A/F)_0=14.7$ )

Another combustion characteristic of a rotary engine is the indicated mean effective pressure (IMEP), which represents the engine output. Figure 12 shows the cycle-to-cycle fluctuations of the IMEP and the A/F ratio near the spark plug at the spark timing. There was a slight correlation between the A/F ratio and IMEP: the IMEP decreased when a leaner mixture existed at the spark timing. However, variations in the IMEP were not very large for IMEPs ranging from 230 to 248 kPa. The IMEP is known to be insensitive to small variations in cycle phasing around MBT (Ozdor et al. 1994). However, this result confirmed that the fuel concentration measured by the spark plug sensor was slightly related to the coefficient of the IMEP variation.

The newly developed spark plug sensor permits us to measure the cycle-to-cycle fluctuations of the fuel concentration around the spark plug in a commercial rotary engine. We could obtain detailed information about the mixture formation process around the spark plug and investigate key features of cyclic variability.

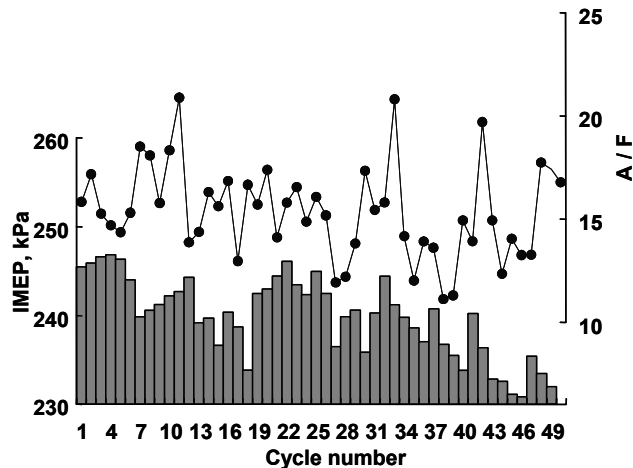


Fig.12 Cyclic fluctuation of the IMEP and the A/F ratio near the spark plug at the spark timing  
( $(A/F)_0=16.1$ )

#### 4. Conclusions

Cycle-resolved measurements of the fuel concentration near the spark plug both in a spark-ignition engine and in a commercial rotary engine were performed using an in-situ laser infrared absorption method with a newly developed optical spark plug sensor. This paper discussed the feasibility of newly developed spark plug sensor in order to understand the mixture formation process and the effects of A/F ratio at the spark timing on the combustion characteristics. The results obtained from this study can be summarized as follows. The developed IR spark plug sensor measured the fuel concentration around a spark plug both in a spark-ignition engine and in a commercial rotary engine quantitatively with high temporal resolution. Strong mixture inhomogeneities were measured during the compression stroke under lean conditions in the rotary engine. The magnitude of these inhomogeneities decreased throughout the compression stroke. There was a strong correlation between the fuel concentration measured with the spark plug sensor and the combustion characteristics during the initial combustion period. The initial combustion was faster when conditions were slightly richer than stoichiometric near the spark plug. The IMEP was slightly related to the A/F ratio near the spark plug. It was possible to measure the cycle-resolved A/F ratio near the spark plug and investigate the cycle-to-cycle fluctuations of this ratio to achieve stable operation under the practical spark-ignition engine using the newly developed spark plug sensor.

#### References

- Egermann, J., Koebecke, W., Ipp, W., and Leipertz, A., (2000) Investigation of the Mixture Formation Inside a Gasoline Direct Injection Engine by Means of Linear Raman Spectroscopy, Proc. Combust. Inst., 28:1145–1152.

- Hall, M. J., and Koenig, M., (1996) A Fiber-Optic Probe to Measure Pre-Combustion In-Cylinder Fuel–Air Ratio Fluctuations in Production Engines, *Proc. Combust. Inst.*, 26:2613–2618.
- Han, D., and Steeper, R. R., (2002) An LIF Equivalence Ratio Imaging Technique for Multicomponent Fuels in an IC Engine, *Proc. Combust. Inst.*, 29:727–734.
- Heywood, J. B., (1988) *Internal Combustion Engine Fundamentals*, McGraw-Hill Book, Inc.
- Jones, C., Harold, C., and Lamping, C., (1971) SAE Paper No.710582.
- Kanbara, S., Noguchi, N., Funamoto, J., Fuse, S., Kashiyama, K., (2003) Mazda Technical Review
- Kawahara, N., Tomita, E., Nishiyama, A., Hayashi, K., (2006) *In-Situ* Fuel Concentration Measurement near Spark Plug by 3.392  $\mu\text{m}$  Infrared Absorption Method (Pressure and Temperature Dependence of the Gasoline Molar Absorption Coefficient), SAE Paper No.2006-01-0182.
- Kawamura, K., Suzuoki, T., Saito, A., Tomoda, T., and Kanda, M., (1998) Development of Instrument for Measurement of Air–Fuel Ratio in Vicinity of Spark-Plug (Application to DI Gasoline Engine), *JSAE Review*, 19(4):305–310.
- Koenig, M., and Hall, M. J., (1997) Measurements of Local In-Cylinder Fuel Concentration Fluctuation in a Firing SI Engine, SAE Paper No. 971644.
- Masaki O. et al., (2004) Development Technologies of the New Rotary Engine(RENESIS), SAE2004-01-1790.
- Muroki, T., Fujimoto, Y., (1987) Unburned Hydrocarbon Emissions of Wankel Type Rotary Piston Engine (1st report, The Source of Unburned Hydrocarbon), *Trans. JSME (in Japanese)*, 53-486, 306-310.
- Muroki, T., (1987) Unburned Hydrocarbon Emissions of Wankel Type Rotary Piston Engine (1st report, Emission Characteristics for Ignition System and Combustion Chamber Shape), *Trans. JSME (in Japanese)*, 53-486, 311-315.
- Nishiyama, A., Kawahara, N., and Tomita, E., (2003) In-Situ Fuel Concentration Measurement near Spark Plug by 3.39  $\mu\text{m}$  Infrared Absorption Method (Application to Spark Ignition Engine), *Trans. SAE - Journal of Engines*, 112-3, (SAE Paper No.2003-01-1109), 1561-1568.
- Nishiyama, A., Kawahara, N., Tomita, E., Fujiwara, M., Ishikawa, N., Kamei, K., Nagashima, K., (2004) in *Situ* Fuel Concentration Measurement near Spark Plug by 3.39  $\mu\text{m}$  Infrared Absorption Method (Application to a Port Injected Lean-Burn Engine), SAE Paper No. 2004-01-1353.
- Ozdor, N., Dulger, M., and Sher, E., (1994) SAE Paper No.940987.
- Rothman, L. S., Rinsland, C. P., Goldman, A., Massie, S. T., Edwards, D. P., Flaud, J.-M., Perrin, A., Camy-Peyret, C., Dana, V., Mandin, J.-Y., Schroeder, J., McCann, A., Gamache, R. R., Wattson, R. B., Yoshino, K., Chance, K. V., Jucks, K. W., Brown, L. R., Nemtchinov, V., and Varanasi, P., (1998) *Journal of Quantitative Spectroscopy and Radiative Transfer*, 60:665–710.
- Shimamura, K., Tadokoro, T., (1981) *Trans. SAE*, SAE Paper No.810277, 1242-1252.
- Shimizu, R., Okimoto, H., Tashima, S., and Fuse, S., (1995) The Characteristics of Fuel Consumption and Exhaust Emissions of the Side Exhaust Port Rotary Engine, *Trans. SAE*, SAE Paper No.950454, 821-828.
- Stone, R., (1999) *Introduction to Internal Combustion Engines 3rd Ed.*, Society of Automotive Engineers, Inc.
- Summers, T., and Collings, N., (1995) Modelling the Transit Time of a Fast Response Flame Ionisation Detector During In-Cylinder Sampling, SAE Paper No. 950160.
- Tadasu H. et al., (2003) Mazda's New Rotary Engine (RENESIS), *Aachener Kolloquium Fahrzeug-und Motorentechnik*.
- Tomita, E., Kawahara, N., Yoshiyama, S., Kakuho, A., Itoh, T., and Hamamoto, Y., (2002) *In-Situ* Fuel Concentration Measurement near Spark-Plug in Spark-Ignition Engines by 3.39  $\mu\text{m}$  Infrared Laser Absorption Method, *Proc. Combust. Inst.*, 29:735–741.
- Tomita E., Kawahara, N., Shigenaga, M., Nishiyama, A., and Dibble, R. W., (2003) *In Situ* Measurement of Hydrocarbon Fuel Concentration Near a Spark Plug in an Engine Cylinder by 3.392  $\mu\text{m}$  Infrared Laser Absorption Method: Discussion of Applicability with a Homogeneous Methane–Air Mixture, *Meas. Sci. Technol.*, 14:1350–1356.
- Tomita, E., Kawahara, N., Nishiyama, A., and Shigenaga, M., (2003) *In Situ* Measurement of Hydrocarbon Fuel Concentration near a Spark Plug in an Engine Cylinder by 3.392  $\mu\text{m}$  Infrared Laser Absorption Method - Application to Actual Engine, *Meas. Sci. Technol.*, 14:1357–1363.
- van Basshuysen, Schäfer, F., (2004) *Internal Combustion Engine Handbook*, Society of Automotive Engineers, Inc.

- Yoshiyama, S., Hamamoto, Y., Tomita, E., and Minami, K., (1996) Measurement of Hydrocarbon Fuel Concentration by Means of Infrared Absorption Technique with 3.39  $\mu\text{m}$  He-Ne Laser, JSAE Review, 17:339-345.
- Zhao, H., and Ladommatos, N., (2001) Engine Combustion Instrumentation and Diagnostics, Society of Automotive Engineers.